Nanoscale Coatings on Wood: Polyelectrolyte Adsorption and Layer-by-Layer Assembled Film Formation

Scott Renneckar*,† and Yu Zhou‡

Department of Wood Science and Forest Products and T. Brooks Forest Products Center, Virginia Tech, Blacksburg, Virginia 24061

ABSTRACT Surface chemistry of wood is based on the exposed surface that is the combination of the intact and cut cellular wall material. It is inherently complex and changes with processing history. Modification of wood surfaces through noncovalent attachment of amine containing water soluble polyelectrolytes provides a path to create functional surfaces in a controlled manner. Adsorption of polyethylenimine (PEI) and polydiallydimethylammonium chloride (PDDA) to wood was quantified as a function of solution conditions (pH and ionic strength). Polycation adsorption was maximized under basic pH without the addition of electrolyte. Added salt either had marginal influence or decreased adsorption of polycation, indicating interactions are strongly influenced by Coulombic forces. PEI adsorption could be modeled by both a Langmuir and Freundlich equations, although the wood surface is known to be heterogeneous. After adsorption of polycations, layer-by-layer assembled films were created on the wood surface. Layered films masked ultrastructural features of the cell wall, while leaving the microscale features of wood (cut lumen walls and openings) evident. These findings revealed for the first time that nanoscale films on wood can be deposited without changing the microscopic and macroscopic texture. Functionalized wood surfaces created by nanoscale films may have a future role in adhesives systems for wood composites, wood protection, and creating new functional features on wood.

KEYWORDS: adsorption • layer-by-layer (LbL) films • wood • polyethyelenimine • functional surfaces

INTRODUCTION

Xylem (wood) is one of the most ancient materials known to man and currently serves as an important and ubiquitous material in our modern society. Wood is primarily composed of cellulose (~40−45 wt %), lignin (~20−32 wt %), and a mixture of heteropolysaccharides known as hemicelluloses (~20−30 wt %) hierarchically organized within a cellular structure (1). When cut, wood tissue is severely heterogeneous based on the chemistries of exposed cell wall polymers, extraneous materials found in wood, and varying scales of surface roughness. Cut wood surface chemistry has been studied using spectroscopy (2, 3), inverse gas chromatography (3, 4), and contact angle analysis (2, 5, 6), which qualifies it as amphoteric and hydrophilic. When the structure of wood is swollen with water, the specific surface area of wood increases 1000 fold from 0.1 to 300 m^2/g (7). Taken together, wood has a nonuniform surface chemistry, with large specific surface area, that is impacted by the mechanical and physical treatments involved during manufacture of forest products. Controlling the surface chemistry of wood may influence the development of new coatings and adhesives for woody and plant-based materials.

In contrast to cut wood surfaces, model biobased films can be created with the utmost control of surface chemistry and architecture by using spin coating (8), Langmuir-Blodgett deposition (9, 10), and layer-by-layer (LbL) adsorption of polyelectrolytes (11−13). Moreover, LbL assembled films are not limited to planer substrates and have been used to engineer the surface of pulp fibers and lignocellulosic fibers, controlling surface chemistry to modify fiber−fiber interactions (14, 15). With these LbL assembled films on fibers, new properties that were difficult to achieve with pulp fiber substrates, such as conductivity, were demonstrated (16).

The formation of multilayers on pulp fibers is an extension of wet-end chemistry of paper science, where irreversible polyelectrolyte adsorption to fiber surfaces was previously revealed (17). Factors that influence polyelectrolyte adsorption onto defined surfaces have been explored from both simulation (18−20) and experimental (21−23) standpoints highlighting segmental charge, surface charge density, and non-ionic interactions affecting the screening enhanced and screening reduced adsorption regimes as a function of electrolyte concentration (24). For these respective two regimes, either (a) the addition of electrolyte mitigates the repulsive forces between like charged segments of a polymer, allowing for a coiled conformation and enhancing adsorption, or (b) interactions between the polymer and surfaces are screened by electrolytes, resulting in decreased adsorption. In both cases, charge neutralization is related to the electrolytes, directly as ions associate with the charged surface, developing the Stern layer (25), or when

* Corresponding author. Phone: (540) 231-7100. Fax: (540) 231-8176. E-mail: srnneck@vt.edu.

Received for review October 14, 2008 and accepted January 7, 2009

† Department of Wood Science and Forest Products, Virginia Tech University.

‡ T. Brooks Forest Products Center, Virginia Tech University.

DOI: 10.1021/am800119q

polymer adsorption occurs releasing adsorbed ions, increasing entropy within the system (26).

Research into the modification of wood-based substrates with polyelectrolytes to control surface chemistry (creation of cationic surfaces) is limited to chemical modification via covalent linkages (27, 28). However, polyethylenimine (PEI) has a history in wood composite research applied as a priming layer for adhesives and was recently investigated in mixtures with reactive biopolymers to form durable cross-linked adhesives (29−31). PEI contains amine functional groups not native to wood that may be used to create a more reactive wood surface. Additionally, PEI is a common polyelectrolyte used as an anchor layer in multilayer films due to its chemistry and structure to facilitate build-up of layer-by-layer films (32). Adsorption of PEI (or other polycations) to wood substrates and the factors that would enhance or inhibit adsorption has not been previously reported. In this study, we investigate the variables that influence polycation adsorption onto wood under a variety of solution conditions and quantify the formation of LbL assembled films onto wood surfaces. Research to understand polycation assembly onto wood substrates will provide a method to systematically engineer the surface of wood with new functional groups.

EXPERIMENTAL SECTION

Materials. Poly(diallyldimethylammonium chloride) (M_w < 100 000), branched poly(ethylenimine) (M_w = 25 000), poly(acrylic acid) (M_w=100,000), poly(allylamine hydrochloride) (PAH, M_w= 70,000), were obtained from Sigma Aldrich. Solutions were prepared using ultra-pure water (Milli-Q Direct 3 UV, Millipore) with a resistivity of 18.2 MΩ · cm. Ionic strength of the solutions was adjusted with NaCl, while pH of the solution was varied with dilute NaOH or HCl. Specimens of different geometries were cut from the sapwood of mature southern yellow pine (*Pinus spp.*) and saturated with water.

Methods. ***Zeta Potential.*** Ground wood samples (140 mesh) were added to ultrapure water (1 % wt/wt) adjusted to a series of pH at 3, 5, 7, 9, 11, and 13. After sedimentation of large particles, the pH of all suspensions were measured and the upper solution containing fine particles were placed in disposable zeta potential cells and analyzed using a Zetasizer Nano ZS (Malvern Instrument Ltd., Worcestershire, U.K.). The same instrument was used to measure the zeta potential of the particles treated with polycation. Samples were prepared by adding 1mg of wood powder to PDDA or PEI solutions (10mg/mL), which were adjusted to a series of pH values of 3, 7, and 10.5 with HCl and NaOH. After 30 min of being stirred, the samples were centrifuged, decanted, and rinsed twice with ultrapure water using the centrifuge. Washed particles were suspended in ultrapure water for zeta potential measurements. A minimum of 5 measurements were taken from duplicate samples for each set of conditions.

CNS Elemental Analysis. Polycation solutions (10mg/mL) were prepared with varying pH (3, 7, and 10.5) and salt contents (0, 0.1, 0.5, 1.0 M). To minimize wood variability between samples, 48 samples were cut from one block to the size of 2.5 × 2.5 × 0.3 cm^3, and two pieces were randomly assigned to each treatment. After saturating the samples with water, each set of flakes were placed in a stirred 100 mL of polycation solution for 24 h. Wood flakes were removed and rinsed with ultrapure water for another 24 h. Wood flakes were dried in a vacuum oven at 40°C for 48 h, ground into particles (60 mesh), and kept dry in a conventional oven at 60°C until measurements. Samples of ground powder (300 mg) were used for elemental analysis (Vario MAX CNS analyzer, Elementar), where samples are combusted and the nitrogen levels are determined by a thermal conductivity detector (sensitivity of 10 ppm nitrogen in helium carrier gas). Similar preparation procedures were followed for adsorption isotherm samples, except wood wafers with the geometry of 1.0 × 1.0 × 0.15 cm^3 were placed in 22°C PEI solutions for 30 min (pH 10.5) followed by rinsing with ultrapure water for 15 min. Note that the average nitrogen content for wood samples was 0.02 % and the nitrogen content for polymer treated species was between 0.04 and o 0.30 %, with an average coefficient of variation of 6 %.

X-ray Photoelectron Spectroscopy. Wood samples were treated with polycation solutions of PEI and PDDA (10mg/mL) with varying pH (3, 7, and 10.5) for 30 min and subsequently rinsed with water for 15 min. The samples were dried in a vacuum oven at 40°C for 48 h. Three replications were included in each condition, and two out of the three were randomly chosen for XPS. Two wood flakes were scanned at an area of 1 mm^2 (PHI Quantera SXM, Scanning Photoelectron Spectrometer Microprobe) for each condition, providing 3 data points for each sample.

Layer-by-Layer Assembly. Layer-by-layer assembled films on wood surfaces were created by sequential treatment of water saturated wood samples (10 cm × 7.5 cm × 0.3 cm) in polyelectrolyte solutions. Solutions of PEI at concentrations of 10 mg/mL, polyacrylic acid (PAA) at 6 mol/mL, and polyallylamine hydrochloride (PAH) at 2.7 mol/L were prepared, respectively. PEI solution pH was adjusted to 10.5, whereas both PAA and PAH solutions were adjusted to pH of 5. Adsorption occurred by placing the samples in 100 mL stirred solutions for 30 min followed by rinsing with water for 15 min between each polyelectrolyte solution. Samples were first treated with PEI and then sequentially treated with PAA and PAH solutions.

Field-Emission Scanning Electron Microscopy. Wood samples treated with the LbL procedure were prepared with three replications for each condition and dried in a vacuum oven at 40°C for 48 h. A 10 nm thick Au/Pd layer was sputter-coated to the specimen with a Kensington sputter coater. A field emission environmental scanning electron microscope (FEI Quanta 600 FEG) was used to image the treated and untreated wood under a vacuum of 0.82 Torr. Duplicate samples were imaged over a magnification range of 100−10 000×, collecting more than 50 images.

Focused Ion Beam Milling. Similar samples to the SEM were prepared and scanned in a FEI Helios 600 Nanolab. Platinum was applied via nozzle injection and a gallium ion emitter (30 kV) was used to mill the selected sample area. Carbon was deposited on the sample externally after milling for added contrast and to reduce charge build-up. Tilt angles of 52° were used to see inside the milled section.

RESULTS AND DISCUSSION

One method that describes the surface charge is the surface potential measurement, which relates the potential at the double layer shear plane to the rest of the solution (25). The zeta potential of ground wood from a group of gymnosperms *Pinus spp*. classified as southern yellow pines was measured using a microelectrophoresis technique. Wood contains an anionic character and to a degree this can be influenced by pH (Figure 1). This result is similar to other systems such as bleached cellulose pulp (partially oxidized), silica, and mica, where deprotonation occurs from surface carboxylic acids or silinol groups (33). The fine particle geometry of ground wood enhances accessibility to the solvent, which may increase this pH effect. A plateau is shown above the pK_a of carboxylic acids; acidic side groups

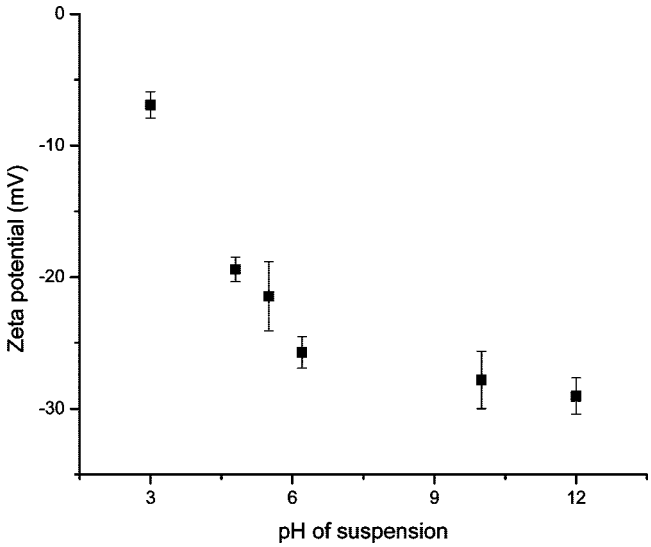

FIGURE 1. Zeta potential of wood particles as a function of solution pH.

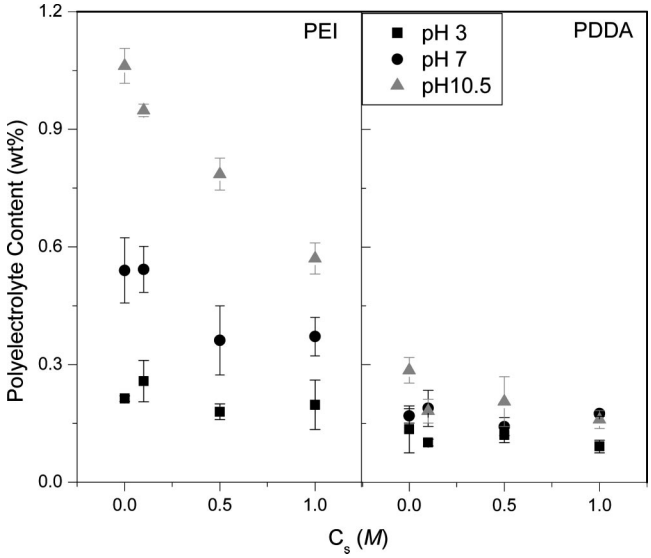

FIGURE 2. Adsorption of polyelectrolyte as a function of salt concentration under different pH ranges.

of aleuronic acid on aribinoglucoronoxylan and galactoronic acid on pectin are the likely candidates that influence the anionic nature of wood. At the highest pH value, the zeta potential approaches −30 mV, when the aromatic biopolymer, lignin, has phenolic groups (0.15−0.3 per phenylpropane unit of softwood) that begin to deprotonate in this alkaline region (1).

Adsorption of polycations to cut wood surfaces is sensitive to both pH and the concentration of NaCl within the solution as measured with elemental analysis (Figure 2). Under alkaline pH, both PEI and PDDA have maximum adsorption in the absence of salt. As salt concentration increases for PEI, there is decreased adsorption under basic pH, whereas no significant decrease in adsorption is found for PDDA above 0.1 M NaCl. PEI adsorption decreases by 10% with the addition of 0.1 M NaCl, whereas PDDA adsorption decreases by 33%. Both of these cases indicate a screening reduced adsorption regime for the polyelectrolytes with higher sensitivity of PDDA to the presence of electrolyte at 0.1 M concentration. When the pH is reduced from 10.0 to 7.0, there is a 40 and 49% reduction of average polymer adsorption for both PDDA and PEI, respectively, in the absence of added electrolyte (Figure 2). For pH 7, increasing the salt content to 0.1 M NaCl showed marginal influence on both PEI and PDDA adsorption. Under acidic pH solution conditions, adsorption is the lowest for the respective polymers and the addition of salt does not influence this result.

Although the zeta potential of wood particles was marginally affected by a reduction in pH from 10.5 to 7 (Figure 1), the degree of segmental charge increases dramatically for PEI (34). PEI contains three times more nitrogen, but it takes on average three times more PEI than PDDA to satisfy the surface charges in alkaline conditions. Charge reduction influences the conformation of the polymer in solution, and the Coulombic interactions between the polymer and the surface. For the charges of the wood surface to be compensated by a weakly charged polyelectrolyte in alkaline solutions, greater polymer adsorption must occur and increased packing of the polymer is facilitated by a coiled conformation (35). PDDA follows a similar trend to PEI: as the pH is decreased from an alkaline solution, the amount of PDDA adsorbed to wood declines. In contrast to PEI, the quaternary ammonium ion of PDDA is still fully charged at the elevated pH, suggesting that other factors besides polymer packing, such as the deprotonation of free phenolic groups within lignin or alkaline induced changes of the wood substrate impact adsorption (36, 37). At reduced pH, the segmental charge of the PEI increases while the surface charge of the wood substrate decreases. There is minimal polymer adsorption when the charge segment density is large and the surface potential is low. For both types of polycations, alkaline pH in the absence of electrolyte maximizes polymer adsorption.

After adsorption of PEI and PDDA to wood substrates, the surface potential of the wood reflects a positive-charged surface as measured using zeta potential in neutral water (Figure 3). The magnitude of surface potential increased as a function of the treating solution pH. A strong correlation is found between the amount of adsorbed polymer and the respective surface potential. Because the surface potential is related to the charge density, the agreement is expected; however, the correlation highlights the impact of an incremental increase in polymer adsorption can have on the surface potential of the substrate. PEI-treated wood samples have a lower corresponding zeta potential relative to PDDA, although PDDA adsorption is overall lower at each corresponding pH (Figure 2). Zheng et al. also report a higher zeta potential for coated pulp fibers under a similar pH when PDDA is the terminal layer of a LbL film relative to PEI (38). Organization and packing of the polyelectrolyte at the surface layers must be different based on polymer chemistry and topology, as PEI is a branched polyelectrolyte. Also, the ratio of charged groups may also affect the data since PEI is a weak polyelectrolyte. XPS measurements highlight a

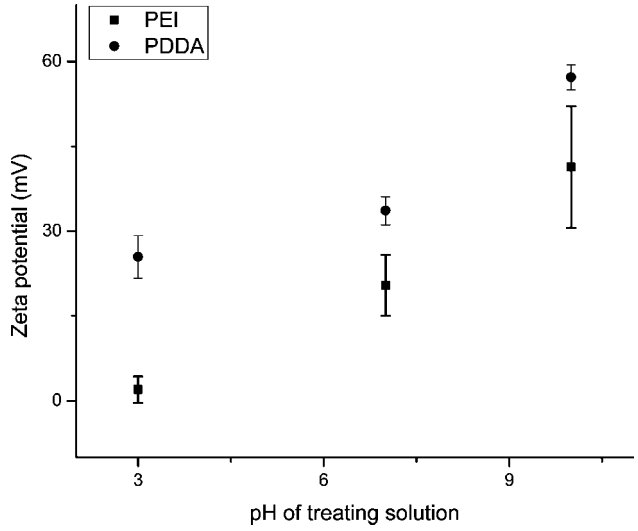

FIGURE 3. Zeta potential of wood particles after adsorption of polyelectrolyte to wood surfaces as a function of treating solution pH. Note: particles were rinsed with, and measurements conducted in, ultrapure water.

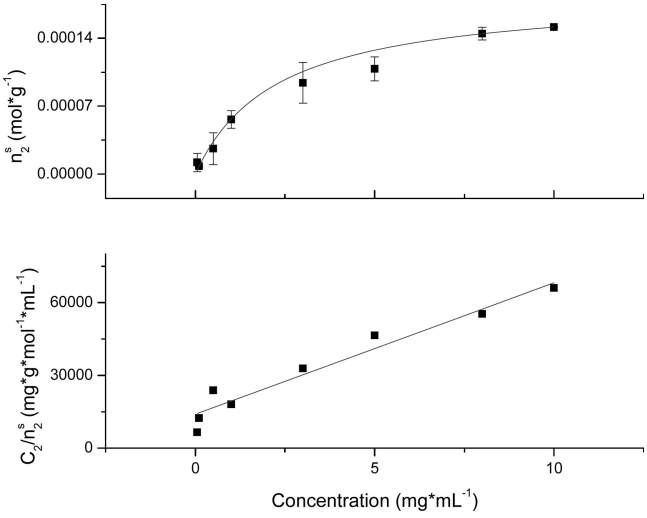

FIGURE 4. Adsorption isotherm of PEI onto wood substrate (pH 10.5). (Top) Data fit to Langmuir equation, (bottom) data fit to eq 1.

combination of ammonium and amine functionalities for PEI-treated wood samples (dried) for solutions of varying pH that were washed in neutral water prior to analysis. Nitrogen detected at the surface of all the samples are in both ammonium form (binding energy of 400.08 eV) and amine form (397.88 eV), which would cause a decrease in the segmental charge of the polymer (see the Supporting Information). However, arising from elemental compositional differences (7.4% N for PDDA and 27.7% N for PEI), nitrogen signals from PDDA-treated wood samples (dried) were not resolved from the baseline signal. Horvath and coworkers used XPS to study PDDA adsorption to pulp fibers and found only 0.5% N signal, highlighting the difficulty of determining PDDA content on lignocellulosic surfaces with XPS (21).

An adsorption isotherm was determined for wood wafers using the condition that provided the largest response based on CNS analysis (PEI, pH 10.5). Increased adsorption is noted as a function of polymer concentration in solution at

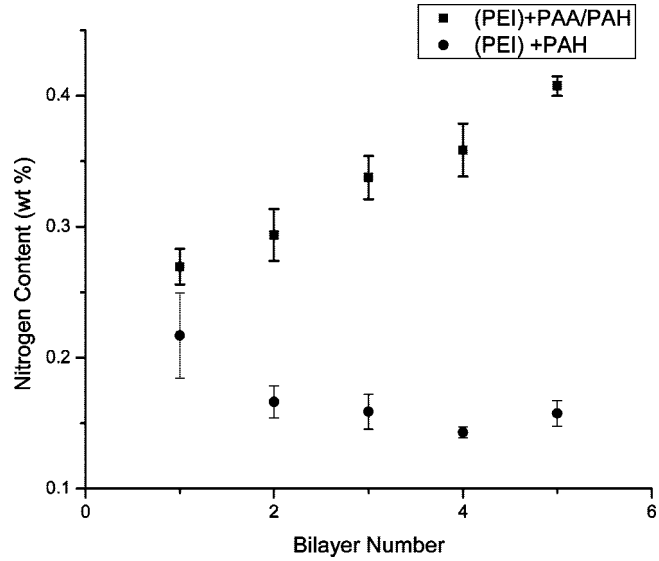

FIGURE 5. Nitrogen content from treated wood samples as a function of the number of soak cycles in polycation solution.

a reduced rate of change. At maximum adsorption (10 mg/mL PEI), polymer concentration is 0.67% of the dry mass of wood (5.86 mg of total PEI). As PEI is only partially depleted from the solution (0.5% is removed), polymer concentration plays a dominate role in controlling adsorption of PEI to the surface within an agitated solution. The affinity coefficient and saturation value was determined from the linear fit of eq 1

$$\frac{C_2}{n^s_2} = \frac{1}{n^s b} + \frac{C_2}{n^s} \quad (1)$$

where C_2 is the solute concentration, n^s_2 is moles of solute adsorbed per gram, b is the Langmuir coefficient related to the intensity of adsorption, and n^s is the adsorption sites per gram (39).

The saturation value (n^s) is 1.86×10^{-4} moles adsorption sites per gram of wood. Given an estimate of PEI size 0.7 mg/m^2 (40) the amount of polymer on the wood surface corresponds to ~11 m^2/g. From the intercept of the line, the Langmuir coefficient was determined to be 0.39 mL mg^{-1}. The Freundlich adsorption model (39) was fitted to the data, providing an affinity coefficient of (0.498) and adsorbent capacity of (4.98×10^{-5} mol/g) with a lower adjusted χ^2 parameter (statistical fitting parameter) than the Langmuir model. Although wood surfaces are known to be heterogeneous, providing justification for the Freundlich model, the data failed the residual analysis because of decreasing trend in the variance.

Thin flakes of wood samples were used for the isotherm with 24 to 27 tracheid cells (1.5 mm) across with a length of 2−3 cells long (1 cm). On the basis of the derived surface area, complete penetration of the polymer into water saturated wood substrate did not occur. Microscopy analysis of wood treated with fluorescently labeled polyelectrolytes under similar conditions confirmed that polyelectrolytes remain at the surface cells for the centrally cut sections (i.e., cells not located at the ends of the sample). This result

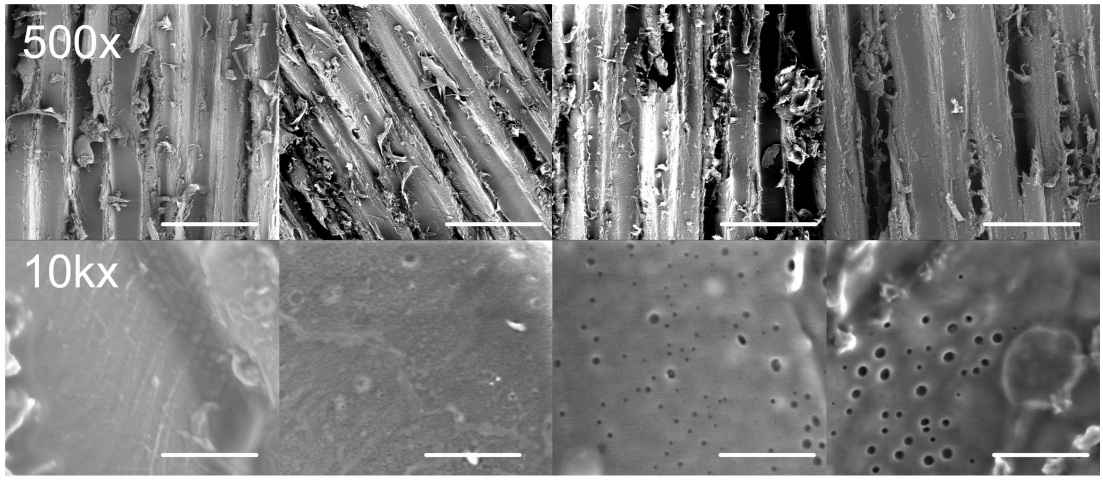

FIGURE 6. SEM images of tangential wood surfaces at low (500×, scale bar 100 μm) and high (10 000×, scale bar 5 μm) magnification. Low-magnification images show the cut cellular nature of wood with its microscale features. High-magnification images show changes in the lumen surface, as multilayer films mask all exposed surfaces.

indicates that polyelectrolytes are not transported below the surface via diffusion through the various micrometer sized openings in the cell wall, keeping a high concentration at the wood wafer surface. Greater penetration of polyelectrolyte would have approached the internal surface area of water saturated wood, which is 10× greater in magnitude (7).

Cut wood surfaces that were treated with a layer of PEI, were sequentially treated with polyacrylic acid (PAA) and polyallylamine hydrochloride (PAH) using layer-by-layer assembly process. A linear build-up of PAA/PAH layers is demonstrated based on the increase in nitrogen content with every soaking cycle of PAH (Figure 5). Past research has shown the influence of pH on layer build-up of weak polyelectrolytes, the amount of polymer adsorbed can be manipulated to suit the desired thickness of the multilayer film (41, 42). For the conditions in the present research, the solution was pH 5 for both PAA and PAH, which would correspond to a thickness of ~8−9 nm per bilayer (42). Without an alternate layer of PAA, the amount of PAH does not increase with subsequent soak cycles (Figure 5). Because of the cellular nature of wood substrates, this data suggests that diffusion controlled adsorption of polyelectrolytes to wood is limited to the exposed surfaces; PAH is not imbibed into the cellular structure after further adsorption cycles. This result suggests that when designing water-saturated wood surfaces using a layer-by-layer procedure, excess polyelectrolyte is not transported away from the surface, and minimal polyelectrolyte is lost during surface functionalization.

Heterogeneity of the cut cellular structure of wood can be seen at low magnification using scanning electron microscopy, where longitudinally arranged cells are found (Figure 6). At 500× magnification, there is no difference among the wood surfaces for all samples. However, at increased magnification, a coating is evident on the lumen cell wall, which has a dimension smaller than the microscale roughness of the wood substrate. Films of $PEI(PAA/PAH)_{1-9}$ can be seen on the cell wall with defects in the films for bilayers of 5 and 9. Morphology of the wood surface begins to change with $PEI(PAA/PAH)_1$ and masks the ultrastructure completely with greater numbers of bilayers (Figure 6). Defects such as submicron sized holes are evident for 5 and 9 bilayers. Surface heterogeneity and the dimensional changes of wood are likely candidates for the cause of the defects found in the film. Lvov and co-workers report the uniformity of LbL coating on wood fibers and found that the surface roughness of the fibers influences the homogeneity of the covering, but after 2−5 layers, homogenous build-up began to occur (43). Similar findings were reported for cotton as a substrate as XPS N/O ratios were used to follow the uniformity of layer structures on cotton, when it took up to 15 layers to show that the substrate no longer influenced the build-up (44). These fiber substrates offer greater uniformity than the wood substrate; however, even in these materials, the submicroscale fiber textures can be seen under the continuous LbL coating (45).

Focus ion beam (FIB) milling was applied to samples coated with 3 and 9 bilayers of PAA and PAH on a PEI treated wood surface (Figure 7A,C). Similarities between the samples are found after cutting the surface; a charging band begins to develop 60 to 250 nm below the surface (Figure 7B,D). Brightness of the band increased as a function of exposure, and because of the increase, the band is attributed to be a potential artifact of the imaging process. The location of the band is not related to the LbL film thickness because of the similarity of the location in the band for both 3 and 9 bilayer samples. It remains unclear if the band corresponds with the layer structure (S3) of the secondary wall of wood tracheid cells. Further investigation of the sample with 9 bilayers was performed by removing the sample and subsequently coating with carbon to help differentiate layer structure. Additional milling behind the initial cut was created to make a membrane slice of the wood (Figure 7E). A dark band is revealed (Figure 7F) in contact with the platinum and the dark layer has a thickness between 40 and 80 nm. The band

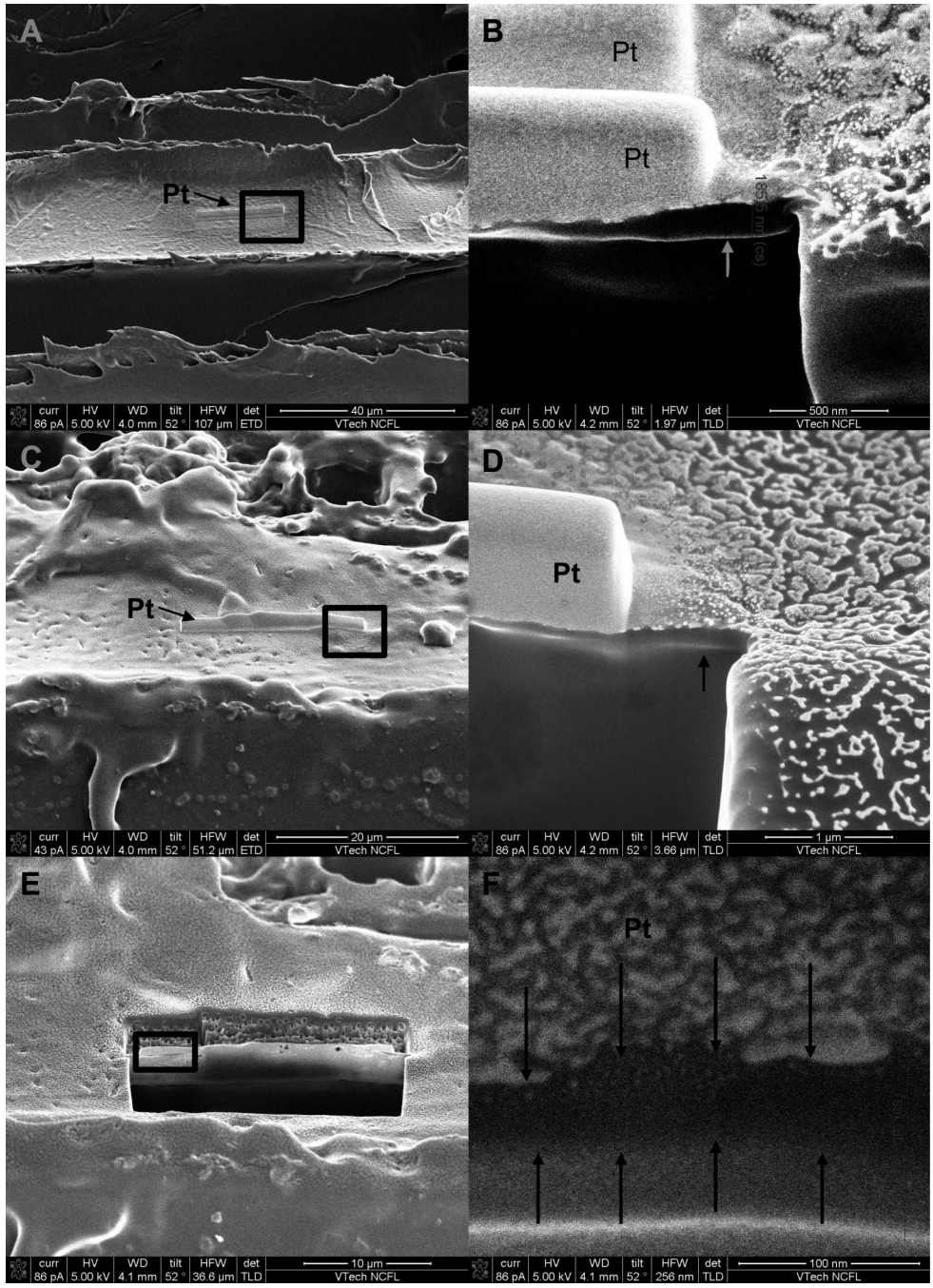

FIGURE 7. FIB images of tangential wood surface with LbL coating (A, B) PEI(PAA/PAH)$_5$ and (C−F) PEI(PAA/PAH)$_9$. (A, C) Overview of wood surface with platinum strip deposited on the surface; (B, D) FIB cut surface revealing the subsurface with a charged layer 30−200 nm below the surface as indicated with the arrow; (E) sample from (D) coated with carbon and material milled from opposite side to form membrane; (F) magnified view of E with the dark band below platinum highlighted by arrows.

matches expectations of LbL film thickness, but because of the difficulties of material contrast, it does not provide direct confirmation of the film size as there is a diffuse halo at the charging line. However, in the lower-magnification images (images A and C in Figure 7), a coated surface is evident and the film must be at the interface of the platinum and the wood. Dejeu and co-workers have used FIB to measure thickness of LbL films deposited upon a silicon wafer with etched silica at the interface and there measurements for 10 bilayers agrees well with laser reflectometry measurements (46). In the present study, the heterogeneous wood surface prohibits identification of the lower boundary of the film for quantitative measurements.

DISCUSSION

Polyelectrolyte adsorption to cellulose-based surfaces has been reported for pulp fibers (47), model cellulose films (9), and natural fibers such as cotton (48). The isolation process of cellulose from its native state typically modifies its chemical functionality (through bleaching processes) influencing porosity, degree of polymerization, and its crystallinity. Hence the surface chemistry amongst cellulose substrates

is unique for the material in question, warranting the investigation of the adsorption process based on different natural substrates. For bleached chemical pulps and regenerated films made from this cellulose source, adsorption of polycations increases in the presence of 0.1 M of added electrolyte (21, 49, 50). When electrolyte is added at concentrations greater than 0.1 M, adsorption is decreased, which is related to the electrostatic charges governing adsorption (screening of electrostatic charges by the salt ions). Wagberg (47) and others (21) reviewed this phenomena for fiber surfaces and related increased adsorption to overcharging the surface (when charge stoichiometry deviates for 1:1); their explanation for the peak in adsorption at 0.1 M of electrolyte is the occurrence of a transition from the mean field approximation of surface charges reducing to point charges on the surface via changes in the Debye length with added electrolyte. At this transition, coiled polyelectrolytes adsorb onto point charges, increasing adsorbed polymer amount, until added electrolyte decreases attraction. In this present study, added electrolyte at 0.1 M for solutions of high pH always decreases the adsorption amount (or remains unchanged for pH 7).

For the wood substrate, there is not an increase in adsorption with any levels of added electrolyte, indicating a different adsorption mechanism than pulp fibers. The difference may arise from a change in the surface charge distribution and/or competitive adsorption of the electrolytes. Scheutjens-Fleer theory for polyelectrolyte adsorption relates adsorption as a function of electrolyte concentration for different levels of secondary interactions and ion competition (51). On the basis of this theory, adsorption regimes for wood substrates follow behavior when ionic interactions dominate with limited contribution from secondary interactions, and/or ion competition occurs with wood surfaces. Although no specific interactions can be attributed to competitive ion adsorption for cellulose pulp surfaces (47), competitive ion adsorption may be relevant for systems containing lignin. Cation$-\pi$ interactions were recently shown to assist in the adsorption mechanism between PDDA and isolated lignins (52). Furthermore, based on computational studies of select cation$-\pi$ binding energies, sodium ions have greater interaction for phenols than ammonium ions have for the same chemical groups (53). Taken together this data would indicate a preference of sodium ions to bind lignin-rich surfaces over ammonium ions of the polymer chains.

Proposed Mechanism of Polyelectrolyte Adsorption to Wood Surfaces. It is clear that the adsorption of polycations to a wood substrate does not follow the same adsorption regime as bleached pulp surfaces. As charge density increases for pulp surfaces, adsorption of polyelectrolyte increases, indicating that adsorption is controlled by the carboxylic acid content of the pulps (47). Chemical composition is a dominate difference between bleached pulp and wood substrates; for wood, the titratable acidic groups, located as branches along the heteropolysaccharides, surround the outer portions of cellulosic fibrils, but are partially masked by lignin. Hence the organization of the polymeric components cause less accessibility to the surface charges on the intact lumen surface, limiting ionic charge to the free phenolics of lignin at elevated pH. A study on polyelectrolyte adsorption to model lignin surfaces indicates added electrolyte decreases adsorption of PDDA onto lignin, as found in the present study, with the majority of the adsorbed polymer bound in close proximity to the surface (54). In another study, it was shown that adsorbed PDDA onto a technical lignin surface had a thickness of 0.5 nm (52). In contrast to the lumen surface, polyelectrolytes adsorbing at the cut cell wall surface have greater access to the hemicellulosic components because the polymeric organization is disrupted. On the basis of the knowledge of how polyelectrolytes adsorb onto the individual components, we propose that adsorption of polyelectrolytes to wood surfaces is dominated by the interactions with the non-cellulosic components and interaction type depends upon the degree of disruption of the wood surface. As polymer adsorption is shown to increase in alkaline pH, available surface charges are increased for wood (titratable free phenolics beginning at pH 8.5). This surface charge creates the need for greater polymer adsorption at higher pH for charge neutralization. At lower pH, adsorption is facilitated through ionic interactions of available carboxylic acid branches of the hemicellulose and pectin components, or by the cation$-\pi$ mechanism that requires close interactions (55) between the ammonium segment and aromatic groups of lignin. In both cases, there are mechanisms that facilitate coverage across the entire wood surface (cut and uncut), providing for noncovalent attachment of polyelectrolytes.

CONCLUSIONS

Irreversible adsorption of polycations to cut wood surfaces can be controlled through careful selection of solution conditions. The zeta potential of the wood particles increased in magnitude with pH, increasing the requirement of charge compensation from oppositely charged polyelectrolytes. This result was highlighted by the occurrence of a maximum in adsorption at elevated pH for both weak and strong polycations. The ionic strength of the solution either had a negative or non-significant effect on adsorption. These results signify that ionic interactions play a dominate role in the adsorption of polycations to wood surfaces. Polyelectrolyte adsorption to wood surfaces is also facilitated by higher concentration of polymers than what is typically reported for ionically assembled monolayers. Although PEI adsorption could be modeled by a Langmuir isotherm, the adsorption plateau was not reached for the concentrations tested of up to 1 % solution by weight. After polyelectrolyte adsorption, the zeta potential of the wood particles reversed to positive values, indicating a cationic surface arising from over charge compensation. With a modified cationic surface, linear build-up of multilayer films after sequential soaking cycles in polyanion and polycation solutions was detected by nitrogen analysis of the samples. Microscopy analysis showed that the film did not mask the microscale features of the wood surface. This study shows that nanoscale films

on wood surfaces were created by the layer-by-layer process, enabling functional wood surfaces with highly controlled surface chemistry.

Acknowledgment. Financial support for this work was provided by the Wood-Based Composite Center and the Sustainable Engineered Materials Institute, which is supported through the USDA-NRI CREES special grants program. Special acknowledgements go to John McIntosh, Stephen McCartney, and Jerry Hunter of the Institute of Critical Technology and Applied Science (ICTAS) Nanoscale Fabrication and Characterization Laboratory for skilled operation and assistance with FIB/SEM/XPS equipments and analysis, and David Mitchem of the Forest Soils Program for training on CNS data collection.

Supporting Information Available: XPS analysis of wood substrates treated with PEI at different pH levels (PDF). This material is available free of charge via the Internet at http://pubs.acs.org.

REFERENCES AND NOTES

(1) Sjostrom, E., *Wood Chemistry Fundamentals and Applications*; Academic Press: San Diego, 1993; p 293.
(2) Sernek, M.; Kamke, F. A.; Glasser, W. G. *Holzforschung* **2004**, *58*, 22.
(3) Liu, F. P.; Rials, T. G.; Simonsen, J. *Langmuir* **1998**, *14*, 536.
(4) Walinder, M. E. P.; Gardner, D. J. *J. Adhes. Sci. Technol.* **2002**, *16*, 1625.
(5) Gindl, M.; Sinn, G.; Gindl, W.; Reiterer, A.; Tschegg, S. *Colloid Surf., A* **2001**, *181*, 279.
(6) Jennings, J. D.; Zink-Sharp, A.; Frazier, C. E.; Kamke, F. A. *J. Adhes. Sci. Technol.* **2006**, *20*, 335.
(7) Stamm, A. J.; Millett, M. A. *J. Phys. Chem.* **1941**, *45*, 43.
(8) Edgar, C. D.; Gray, D. G. *Cellulose* **2003**, *10*, 299.
(9) Tammelin, T.; Saarinen, T.; Oesterberg, M.; Laine, J. *Cellulose* **2006**, *13*, 519.
(10) Gradwell, S. E.; Renneckar, S.; Esker, A. R.; Heinze, T.; Gatenholm, P.; Vaca-Garcia, C.; Glasser, W. *C. R. Biol.* **2004**, *327*, 945.
(11) Renneckar, S.; Zink-Sharp, A.; Esker, A. R.; Johnson, R. K.; Glasser, W. G. Novel methods for interfacial modification of cellulose-reinforced composites. In *Cellulose Nanocomposites: Processing, Characterization, and Properties*; Oksman, K., Sain, M., Eds.; American Chemical Society: Washington, D.C., 2006; Vol. 938, p 78.
(12) Cranston, E. D.; Gray, D. G. *Biomacromolecules* **2006**, *7*, 2522.
(13) Podsiadlo, P.; Choi, S.-Y.; Shim, B.; Lee, J.; Cuddihy, M.; Kotov, N. A. *Biomacromolecules* **2005**, *6*, 2914.
(14) Lingstrom, R.; Wagberg, L.; Larsson, P. T. *J. Colloid Interf. Sci.* **2006**, *296*, 396.
(15) Wagberg, L.; Forsberg, S.; Johansson, A.; Juntti, P. *J. Pulp Pap. Sci.* **2002**, *28*, 222.
(16) Agarwal, M.; Lvov, Y.; Varahramyan, K. *Nanotechnology* **2006**, *17*, 5319.
(17) Allan, G. G.; Akagane, K.; Neogi, A. N.; Reif, W. M.; Mattila, T. *Nature* **1970**, *225*, 175.
(18) Kong, C. Y.; Muthukumar, M. *J. Chem. Phys.* **1998**, *109*, 1522.
(19) Carrillo, J.-M. Y.; Dobrynin, A. V. *Langmuir* **2007**, *23*, 2472.
(20) Borukhov, I.; Andelman, D.; Orland, H. *Macromolecules* **1998**, *31*, 1665.
(21) Horvath, A. E.; Lindström, T.; Laine, J. *Langmuir* **2006**, *22*, 824.
(22) Winkler, R. G.; Cherstvy, A. G. *J. Phys. Chem. B* **2007**, *111*, 8486.
(23) Blaakmeer, J.; Bohmer, M. R.; Stuart, M. A. C.; Fleer, G. J. *Macromolecules* **1990**, *23*, 2301.
(24) Van de Steeg, H. G. M.; Stuart, M. A.; De Keizer, A.; Bijsterbosch, B. H. *Langmuir* **1992**, *8*, 2538.
(25) Evans, D. F.; Wennerstrom, H., *The Collodial Domain*; Wiley-VCH: Weinheim, Germany, 1999.
(26) Ariga, K.; Hill, J. P.; Ji, Q. *Phys. Chem. Chem. Phys.* **2007**, *9*, 2319.
(27) Karthikeyan, K. G.; Tshabalala, M. A.; Wang, D.; Kalbasi, M. *Environ. Sci. Technol.* **2004**, *38*, 904.
(28) Baouab, M. H. V.; Gauthier, R.; Gauthier, H.; El Baker Rammah, M. *J. Appl. Polym. Sci.* **2001**, *82*, 31.
(29) Geng, X.; Li, K. *J. Adhes. Sci. Technol.* **2006**, *20*, 847.
(30) Li, K.; Geng, X. *Macromol. Rapid Commun.* **2005**, *26*, 529.
(31) Li, K.; Geng, X.; Simonsen, J.; Karchesy, J. *Int. J. Adhes. Adhes* **2004**, *24*, 327.
(32) Kolasinska, M.; Krastev, R.; Warszynski, P. *J Colloid Interf. Sci.* **2007**, *305*, 46.
(33) Stemme, S. *Factors Influencing Polyelectrolyte Conformation at a Cellulose Model Surface and at a Silica Surface*. Kungl Tekniska Hogskolan: Stockholm, Sweden, 1996.
(34) Griffiths, P. C.; Paul, A.; Stilbs, P.; Petterson, E. *Macromolecules* **2005**, *38*, 3539.
(35) Meszaros, R.; Thompson, L.; Bos, M.; de Groot, P. *Langmuir* **2002**, *18*, 6164.
(36) Stamm, A. J. *J. Am. Chem. Soc.* **1934**, *56*, 1195.
(37) Mantanis, G. I.; Young, R. A.; Rowell, R. M. *Holzforschung* **1995**, *49*, 239.
(38) Zheng, Z. G.; McDonald, J.; Khillan, R.; Su, Y.; Shutava, T.; Grozdits, G.; Lvov, Y. M. *J. Nanosci. Nanotechnol.* **2006**, *6*, 624.
(39) Adamson, A. W.; Gast, A. P. *Physical. Chemistry of Surfaces*; Wiley: New York, 1997; p 784.
(40) Aulin, C.; Varga, I.; Claesson, P. M.; Wagberg, L.; Lindström, T. *Langmuir* **2008**, *24*, 2509.
(41) Yoo, D.; Shiratori, S. S.; Rubner, M. F. *Macromolecules* **1998**, *31*, 4309.
(42) Choi, J.; Rubner, M. F. *Macromolecules* **2005**, *38*, 116.
(43) Lvov, Y. M.; Grozdits, G. A.; Eadula, S.; Zheng, Z.; Lu, Z. *Nord. Pulp Pap. Res. J.* **2006**, *21*, 552.
(44) Hyde, K.; Dong, H.; Hinestroza, J. P. *Cellulose* **2007**, *14*, 615.
(45) Lu, Z.; Eadula, S.; Zheng, Z.; Xu, K.; Grozdits, G.; Lvov, Y. *Colloid Surf., A* **2007**, *292*, 56.
(46) Dejeu, J.; Salut, R.; Spajer, M.; Membrey, F.; Foissy, A.; Charraut, D. *Appl. Surface Sci.* **2008**, *254*, 5506.
(47) Wagberg, L. *Nord. Pulp Pap. Res. J.* **2000**, *15*, 586.
(48) Hyde, K.; Rusa, M.; Hinestroza, J. *Nanotechnology* **2005**, *16*, 422.
(49) Horvath, A. T.; Horvath, A. E.; Lindstrom, T.; Wagberg, L. *Langmuir* **2008**, *24*, 10797.
(50) Horvath, A. T.; Horvath, A. E.; Lindström, T.; Wagberg, L. *Langmuir* **2008**, *24*, 7857.
(51) Fleer, G. J.; Stuart, M. A.; Scheutjens, J. M. H. M.; Cosgrove, T.; Vincent, B., *Polymers at Interfaces*; Springer: New York, 1993; p 520.
(52) Pillai, K.; Renneckar, S. *Biomacromolecules* **2009**, In press.
(53) Ma, J. C.; Dougherty, D. A. *Chem. Rev.* **1997**, *97*, 1303.
(54) Norgren, M.; Gaerdlund, L.; Notley, S. M.; Htun, M.; Wagberg, L. *Langmuir* **2007**, *23*, 3737.
(55) Gallivan, J. P.; Dougherty, D. A. *J. Am. Chem. Soc.* **2000**, *122*, 870.

AM800119Q